# Neutron Cross Sections for Some Threshold Reactions

TORBJÖRN LAGERWALL

Hahn-Meitner-Institut für Kernforschung, Berlin, and Chalmers University of Technology, Göteborg *

(Z. Naturforschg. **20 a**, 1583—1587 [1965]; received 3 September 1965)

Three neutron reactions leading to production of the rare gases $Ar^{41}$ and $Xe^{135}$ have been investigated. Single crystal samples of KF, $CaF_2$, and $BaF_2$ were irradiated in the Berlin reactor and the target-free absolute activities of the rare gas isotopes measured by a $\beta$-$\gamma$-coincidence method. The calculated cross sections are

| | | |
|---|---|---|
| $K^{41}(n,p)Ar^{41}$: | $\sigma = (2{,}73 \pm 0{,}41)$ mb; | $\sigma_0 = (98{,}6 \pm 14{,}8)$ mb; |
| $Ca^{44}(n,\alpha)Ar^{41}$: | $\sigma = (61{,}1 \pm 9{,}2)$ $\mu$b; | $\sigma_0 = (64{,}7 \pm 9{,}7)$ mb; |
| $Ba^{138}(n,\alpha)Xe^{135}$: | $\sigma = (1{,}9 \pm 0{,}3)$ $\mu$b; | $\sigma_0 = (4{,}9 \pm 0{,}7)$ mb. |

The first set of values are valid for a fission-neutron spectrum. The second set are calculated cross sections for the high energy plateau. They can be considered as valid for 15 MeV neutrons.

## 1. General Considerations

Radioactive rare gases can be produced from alkali and alkaline earth compounds by (n,p)- and (n,$\alpha$)-reactions respectively. In this work the reactions

(i) $K^{41}(n,p)\,Ar^{41}(110\text{ min})$ [1,8 MeV]
(ii) $Ca^{44}(n,\alpha)\,Ar^{41}(110\text{ min})$ [2,8 MeV]
(iii) $Ba^{138}(n,\alpha)\,Xe^{135}(9{,}2\text{ hours})$ [$-3{,}8$ MeV]

(figures in brackets relate to half-live and reaction thresholds)

have been studied using the fast flux of the Berlin Experimental Research (BER) reactor. As the fast neutron distribution is known with good accuracy at the irradiation position, a homogeneous reactor of the BER type is well suited for cross section measurements of threshold reactions.

Let $\sigma(E)$ be the microscopic cross section for the reaction at energy $E$, $\Phi(E)$ the neutron flux density at energy $E$, $N$ the number of target atoms in the sample, $T$ the irradiation time in the reactor, and $\lambda$ the decay constant of the produced rare gas isotope, then the activity $A$ of the rare gas in the sample at the time $t$ after withdrawal of the sample from the reactor is given by

$$A = \lambda N (1 - e^{-\lambda T})\, e^{-\lambda t} \int_{E_T}^{\infty} \Phi(E)\, \sigma(E)\, \mathrm{d}E \quad (1)$$

where $E_T$ designates the threshold energy for the reaction. Because of the reaction threshold, a measurement of the absolute activity $A$ will furnish a value of the cross section which may, under certain conditions, be valid for an unmoderated fission spectrum, and further make possible an evaluation of the cross section at high energies.

In order to show this, the GAMOW factors for the reactions have been calculated and are plotted as functions of energy in Fig. 1. They give the transparency of the COULOMB barriers from the threshold

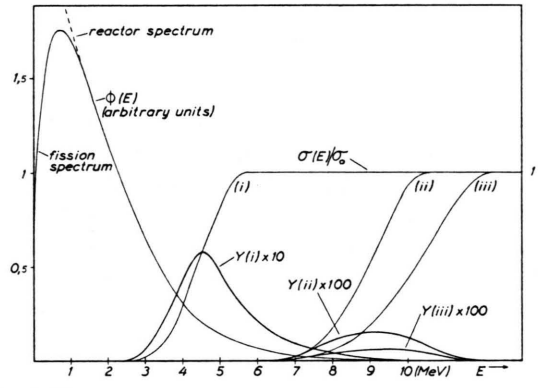


Fig. 1. Energy spectrum of the fast neutrons in the centre of the BER reactor core plotted together with the normalized cross sections for the investigated reactions as described by the GAMOW factor (fine lines). The products of neutron flux density and cross section are also shown (heavy lines).

energy up to high energies at which the cross section has reached the saturation value $\sigma_0$, which can be regarded as constant in the region 10 to 20 MeV within good approximation [1]. In the same figure the neutron energy spectrum in the centre of the reactor core is given. At energies above 1 MeV the devia-

* Present address: Institute of Physics, Chalmers University of Technology, Göteborg, Sweden.

[1] P. M. UTHE, USA FIT-TR-57-3 [1957].

tions of the reactor spectrum from a pure fission spectrum are small and can be neglected at 2 MeV and higher [2].

As reactions (i) and (ii) have threshold energies in the MeV-range, moderated neutrons cannot be expected to make important contributions to the reaction yield. Due to the height of the COULOMB barrier this is, however, also true for (iii) even though this reaction is strongly exothermic. At 3 MeV, for instance, the GAMOW factor amounts to $5 \cdot 10^{-8}$. On regarding the integrand function in eq. (1) which has also been traced in Fig. 1, it is seen that neutrons below 2,5 MeV do not contribute to reaction (i). For reactions (ii) and (iii) neutrons below about 6 MeV do not contribute.

The lower limit of the integral in eq. (1) can then be extended down to zero without affecting the value of $A$. On introducing the abbreviations

$$\Phi = \int_0^\infty \Phi(E)\, \mathrm{d}E \tag{2}$$

and

$$\sigma = \frac{\int_0^\infty \Phi(E)\, \sigma(E)\, \mathrm{d}E}{\int_0^\infty \Phi(E)\, \mathrm{d}E}, \tag{3}$$

eq. (1) can be written as

$$A = \lambda N (1 - e^{-\lambda T})\, e^{-\lambda t} \cdot \Phi \cdot \sigma \tag{4}$$

where $\Phi$ now stands for the integrated fission-neutron spectrum and $\sigma$ for the fission-neutron cross section of the reaction. As the reasoning above has shown that only unmoderated neutrons are effective in all three investigated reactions, eq. (4) is valid although $\Phi$ and $\sigma$ relate to the pure fission spectrum whereas $A$ relates to the actual reactor spectrum.

Two graphs facilitating the calculations of GAMOW factors for nuclear reactions are given in the Appendix.

## 2. Experimental Technique

Single crystals of optical quality of KF (Korth), $CaF_2$ and $BaF_2$ (Harshaw) were used. Samples of 0,5 to 5 g were irradiated in the central position of the core for 1 to 2 hours. After irradiation the crystal was induction heated to melting (1400 – 1500 °C) under vacuum in a graphic crucible and the escaped rare gas was collected on an activated charcoal trap at liquid air temperature. By heating the trap, the total amount of gas was then transferred into an evacuated counting chamber, shown in Fig. 2. Because the gas activity is readily separated from (n,$\gamma$)-induced activities in the target substance, all irradiations could be made without wrapping the sample in cadmium, thus avoiding flux depression at the irradiation position.

The cylindrical brass chamber in Fig. 2 had walls of 0,4 cm thickness except for one of the circular end-faces which had a 0,005 cm thin aluminium window for $\beta$-counting. The absolute activity $A$ of the gas in the chamber was determined by a $\beta$-$\gamma$-coincidence measurement. A 3,2 × 0,6 cm anthracene crystal and a 5 × 5 cm NaJ(Tl) crystal (Harshaw Integral Line) were used. The counting chamber was placed close to the anthracene crystal and 50 to 200 cm away from the NaJ-crystal as shown in the figure. In this way the efficiency can be regarded as independent of the position of the decaying atom within the counting chamber. The decay schemes of the two measured isotopes are shown in Fig. 3 and further discussed in the next section.

The resolving time for the coincidence channel was $\vartheta = 0{,}5\ \mu s$ and for the $\beta$- and $\gamma$-channels $\tau = 10\ \mu s$.

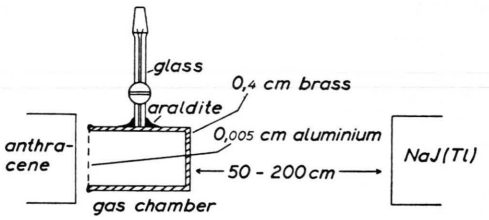


Fig. 2. Arrangement for $\beta$-$\gamma$-coincidence counting. The gas chamber has 4 cm diameter and 6 cm length. The scintillation crystals have the dimensions 3,2 × 0,6 cm (anthracene) and 5 × 5 cm (NaJ). The distance between counting chamber and $\beta$-scintillator was about 1 cm, that between counting chamber and $\gamma$-scintillator varied according to the strength of the gas sample.

## 3. Calculation of the Decay Rate

Let $R'_\beta$, $R'_\gamma$ and $R'_{\beta\gamma}$ designate the measured counting rates at a certain moment in the $\beta$-, $\gamma$- and coincidence channels respectively, and let the same symbols without prime indices stand for the corresponding rates after correction for background ($\gamma$ and $\beta$) and accidental coincidence rate. As $(R'_\beta + R'_\gamma)\, \vartheta \ll 1$ in all experiments, the accidental coincidence rate is given by the approximate expression [3] $2\, \vartheta\, R'_\beta R'_\gamma$. As further $R_{\beta\gamma} \cdot \tau \ll 1$ no dead time corrections had to be made [4]. Then, apart

[2] D. J. HUGHES, Pile Neutron Research, Addison-Wesley, Cambridge 1953, p. 100.

[3] P. J. CAMPION, Intern. J. Appl. Radiation Isotopes **4**, 237 [1959].

[4] G. WOLF, Nukleonik **2**, 258 [1961].

[5] J. L. PUTMAN, AERE 1/M 26 [1953].

from corrections to be discussed below, the absolute decay rate is given by (see e. g. [5] or standard textbooks)

$$A = (R_\beta \cdot R_\gamma)/R_{\beta\gamma} . \qquad (5)$$

The counts were taken simultaneously in the three channels and the measuring time varied in different experiments from 10 to 60 minutes during which time the decay cannot be neglected. If $Z$ is the total number of counts observed in any channel during the measuring time $t_m$

$$Z = \int_0^{t_m} R(t)\, dt = R(0) \int_0^{t_m} e^{-\lambda t}\, dt , \qquad (6)$$

and hence

$$R(0) = \frac{Z}{t_m} \cdot \frac{\lambda t_m}{1 - e^{-\lambda t_m}} . \qquad (7)$$

The value $R(0)$, the counting rate at the beginning of the measurement, was used in eq. (5).

As can easily be shown [6], no correction has to be made due to the branching in the decay schemes, provided that either the $\beta$- or the $\gamma$-efficiencies are the same for both branches. This condition is fulfilled, as the $\beta$-efficiency is energy independent for the occurring energies. PUTMAN has further shown [5] that the finite size of the sample leaves eq. (5) unaffected if either the $\beta$- or the $\gamma$-efficiency is independent of the position of the decaying atom in the sample, a condition which is approximately fulfilled for the $\gamma$-counting in the arrangement shown in Fig. 2. Neither is a correction for angular correlation necessary. The 1,20 MeV $\beta$ transition of $Ar^{41}$ has a comparative half life $ft$ for which $\log ft = 5{,}0$ and for the 0,91 MeV transition of $Xe^{135}$ $\log ft$ can be estimated to 5,8. Thus both transitions are allowed and the $\beta$-$\gamma$-distribution is isotropic. Then only such corrections have to be applied, which account for internal conversion, the $\gamma$-efficiency of the $\beta$-detector, bremsstrahlung quanta produced in the walls of the counting chamber, and the presence of other rare gas isotopes.

The consideration of these factors leads to the expression

$$\frac{R_\beta \cdot R_\gamma}{R_{\beta\gamma}} = A(1+\zeta)(1+\eta)(1+2b) \qquad (8)$$

where the corrections $\zeta$, $\eta$, and $b$, normally of the order 1 to 5 per cent, will be discussed in the following.

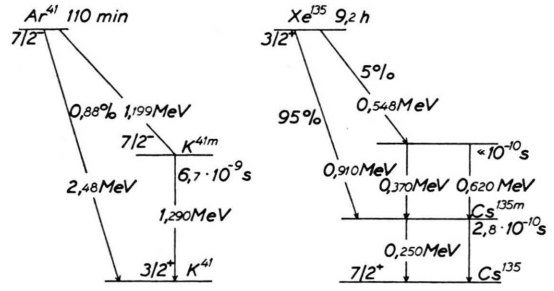


Fig. 3. Decay schemes of $Ar^{41}$ and $Xe^{135}$. (From A. SCHWARZSCHILD, B. M. RUSTAD, and C. S. WU, Phys. Rev. **103**, 1796 [1956], and D. STROMINGER, J. M. HOLLANDER, and G. T. SEABORG, Rev. Mod. Phys. **30**, 653 [1958].)

### *a) Internal Conversion*

Conversion of the $\gamma$-rays leads to a decrease of $R_\gamma$ and $R_{\beta\gamma}$ and an increase of $R_\beta$. If $p_\beta$ is the $\beta$-counting efficiency, which for the given geometrical arrangement is of the order of 5 per cent, $\alpha_1$ and $\alpha_2$ the conversion coefficients of the respective branches and if $a$ is the branching ratio (0,9 per cent for $Ar^{41}$, 5 per cent for $Xe^{135}$), straightforward reasoning gives the correction factor for $A$ in eq. (5),
for $Ar^{41}$

$$1 + \zeta = 1 + (1-a)(1-p_\beta)\,\alpha \approx 1 + \alpha ; \qquad (9)$$

for $Xe^{135}$

$$1 + \zeta = 1 + (1-p_\beta)[(1-a)\,\alpha_1 + a\,\alpha_2] \approx 1 + \alpha_1 . \qquad (10)$$

For $Ar^{41}$ the M2-transition of 1,3 MeV has a conversion coefficient $\alpha < 10^{-4}$ whereas $\alpha_1$ for the 0,250 MeV (E2 or M1) transition in $Xe^{135}$ is equal to 0,06 [7].

### *b) $\gamma$-efficiency of the $\beta$-detector*

From the known $\gamma$-ray absorption coefficient of anthracene [8] (0,074 $cm^{-1}$ and 0,150 $cm^{-1}$ for 1,3 MeV and 0,250 MeV respectively) the $\gamma$-efficiency $\eta$ of the anthracene was calculated to 0,03 ($Ar^{41}$) and 0,06 ($Xe^{135}$). The effect increases $R_\beta$, and $A$ should be corrected with the factor $(1+\eta)$.

[6] See, e. g., J. L. PUTMAN, AERE N/R 318 [1949].
[7] R. D. EVANS, The Atomic Nucleus, McGraw-Hill, New York 1955, pp. 215, 619.
[8] K. SIEGBAHN (ed.), $\beta$- and $\gamma$-Ray Spectroscopy, North-Holland Publishing Co., Amsterdam 1955, p. 152.

*c) Contribution of Bremsstrahlung*

The number of $\gamma$-quanta $b$ created in the brass per $\beta$-particle can be calculated from the thick target bremsstrahlung intensity formula [7]

$$I = \frac{Z}{7000} E_0^2 \,\mathrm{MeV}(\gamma)/\beta\text{-decay} \qquad (11)$$

together with an estimation of the average energy of the $\gamma$-quantum. As is easily seen, the correction factor for $A$ due to bremsstrahlung quanta is $(1+2\,b)$, where the factor 2 accounts for the fact that weak quanta ($\bar{E} \approx 200-300$ keV) are detected with twice the efficiency of 1 MeV quanta. The estimated values of $b$ were 0,024 for $Ar^{41}$ and 0,017 for $Xe^{135}$.

*d) Presence of Other Rare Gas Isotopes*

In the $CaF_2$ irradiation, apart from $Ar^{41}$ the 34 days $Ar^{37}$ was also created and identified by its half-life. Decaying by electron capture, it is detected by its internal bremsstrahlung. According to the MORRISON–SCHIFF formula [9] the ratio of photon emission and electron capture is

$$\lambda_\gamma/\lambda_{EC} = \frac{\alpha}{12\,\pi}\,(E_0/m_0\,c^2)^2, \qquad (12)$$

where $\alpha$ is the fine structure constant, $m_0\,c^2$ the electron rest energy and $E_0$ the reaction energy. Estimating the reaction cross section for the creation of $Ar^{37}$ from HUGHES' theory [2] and taking into account the high detecting efficiency for the average energy ($\sim 200$ keV) quanta, the contribution to $R_\gamma$ from $Ar^{37}$ is estimated to be slightly less than 1 per cent. However, $\gamma$-measurements after complete decay of $Ar^{41}$ showed that about 7 per cent of the initial $\gamma$-rate was due to this isotope. Formally, the correction for this can be contained in the value of $2\,b$ which then amounts to 0,12 for $Ar^{41}$. In the $BaF_2$ irradiation the measured contribution of the 5,6 days $Xe^{133}$ to the total activity was slightly larger than 1 percent, which well agreed with the estimated value.

No corrections for crystal impurities have been introduced above and are, in fact, necessary. The only critic atomic impurity, which is $K$ in $CaF_2$, was present in less than 0,005% in the crystals used.

## 4. Results

The order of magnitude of the measured activities can be seen from Table 1, where the total number of counts $Z$ in the $\beta$-, $\gamma$-, and coincidence channels are given together with the corresponding values of the pertaining quantities in eq. (4).

Combining eqs. (4) and (8) with the value of the fission neutron flux, $\Phi = 8{,}7 \cdot 10^{11}$ cm$^{-2}$ s$^{-1}$, in the middle of the reactor core gave the values

(i) $K^{41}(n,p)Ar^{41}$: $\sigma = (\ 2{,}73 \pm 0{,}41)$ mb;
(ii) $Ca^{44}(n,\alpha)Ar^{41}$: $\sigma = (61{,}1\ \pm 9{,}2\ )\ \mu$b;
(iii) $Ba^{138}(n,\alpha)Xe^{138}$: $\sigma = (\ 1{,}9\ \pm 0{,}3\ )\ \mu$b.

These are average values based on three runs for reaction (ii) and on two runs for the other reactions. The main part of the probable error given is due to the uncertainty in the absolute value of the integrated fission flux (corresponding to a standard deviation of 20 per cent in that quantity). The cross section values calculated on the basis of the approximate theory by HUGHES are 7 mb, 100 $\mu$b and 30 $\mu$b for reactions (i), (ii), and (iii), respectively. No experimental data have been reported in the literature. In activation calculations based on the values given above the fission flux $\Phi$ can for most reactors be taken as approximately equal to the thermal flux, provided that the irradiation is made in the centre of a homogene-

| Reaction | $\Phi$ (cm$^{-2}$ s$^{-1}$) | $N$ | $T$ (min) | $t$ (min) | $Z_\beta$ | $Z_\gamma$ | $Z_{\beta\gamma}$ | $t_m$ (min) |
|---|---|---|---|---|---|---|---|---|
| (i) | $8{,}7 \cdot 10^{11}$ | $2{,}42 \cdot 10^{20}$ | 92 | 285 | 941 753 | 654 673 | 20 291 | 10 |
| | | $3{,}20 \cdot 10^{21}$ | 122 | 205 | 1 784 741 | 1 908 225 | 8 253 | 15 |
| (ii) | $8{,}7 \cdot 10^{11}$ | $3{,}77 \cdot 10^{20}$ | 122 | 190 | 427 202 | 175 432 | 9 548 | 60 |
| | | $2{,}57 \cdot 10^{21}$ | 92 | 140 | 515 452 | 147 934 | 8 613 | 15 |
| | | $3{,}77 \cdot 10^{20}$ | 122 | 170 | 152 853 | 58 144 | 3 145 | 15 |
| (iii) | $8{,}7 \cdot 10^{11}$ | $1{,}04 \cdot 10^{22}$ | 93 | 310 | 50 013 | 55 438 | 1 931 | 15 |
| | | $2{,}35 \cdot 10^{21}$ | 93 | 255 | 25 057 | 32 517 | 1 542 | 20 |

Table 1.

[9] P. MORRISON and L. SCHIFF, Phys. Rev. **58**, 24 [1940].

ous type reactor or alternatively within or close to a fuel rod in a heterogeneous type reactor. If the irradiation position is situated midway between two fuel rods, the value is normally lower by about one order of magnitude.

From the measured cross sections and the known neutron energy distribution in the reactor core it is possible to evaluate the saturation values $\sigma_0$ of the cross sections at higher energies.

On writing

$$\sigma \cdot \Phi = \sigma_0 \int_0^\infty \Phi(E)\ \sigma(E)/\sigma_0\, \mathrm{d}E = \sigma_0 \cdot Y \qquad (13)$$

and thus

$$\sigma_0 = \sigma \cdot \Phi / Y\,, \qquad (14)$$

a comparison of the areas under the $\Phi(E)$-curve and the $\Phi(E)\ \sigma(E)/\sigma_0$-curve in Fig. 1 will give the plateau value. The comparison was made by graphical integration, and an accurate plot of the $\Phi(E)\ \sigma(E)/\sigma_0$-curves was provided by using the data on spectral distribution $\Phi(E)$ by SCHOPPER [10]. The results of this evaluation are

(i) $K^{41}(n,p)Ar^{41}$: $\sigma_0 = (98{,}6 \pm 14{,}8)$ mb;

(ii) $Ca^{44}(n,\alpha)Ar^{41}$: $\sigma_0 = (64{,}7 \pm 9{,}7)$ mb;

(iii) $Ba^{138}(n,\alpha)Xe^{134}$: $\sigma_0 = (4{,}9 \pm 0{,}7)$ mb.

The first of these values can be compared with the value $(81 \pm 31)$ mb for the same reaction at 14,5 MeV reported by PAUL and CLARKE [11]. Their value was calculated from a $\beta$-measurement with an estimated counter efficiency. No details of the preparation of gas samples were given. For the other reactions literature data are lacking.

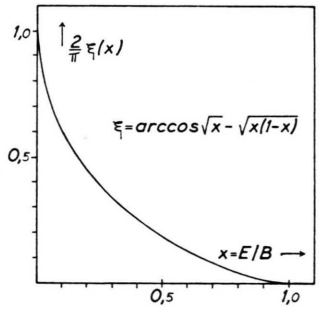


Fig. 4. Parameter $(2/\pi)\ \xi$ in GAMOW factor as a function of the ratio of excitation to COULOMB barrier energy. The excitation energy is with good approximation equal to the neutron energy in excess of the reaction threshold.

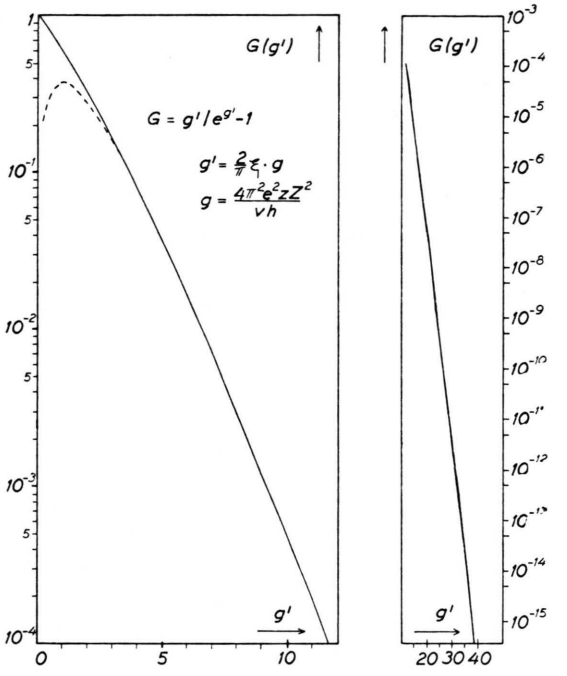


Fig. 5. GAMOW factor (transparency of COULOMB potential barrier) for nuclear reactions. $e$ is the electronic charge, $h$ the PLANCK constant, $z$ and $Z$ atomic number of emitted particle and product nucleus respectively and $v$ velocity of emitted particle. $(2/\pi)\ \xi$ can be taken from Fig. 4. Dashed curve shows the approximation $G = g' \cdot e^{-g'}$. If $E$ is the excitation energy in keV and $a$ the mass number of the emitted particle, a convenient expression for calculations is $g = 31{,}5\ z\, Z \sqrt{a/E}$.

*Acknowledgements*

The author wishes to express his appreciation to Dr. H. BUCHHOLZ for kindly placing his spectrometer equipment at the author's disposal. Mr. W. LEUTHER assisted skillfully in the measurements. Thanks are also due to the reactor irradiation service at the Hahn-Meitner-Institute and to Professors K. E. ZIMEN, Berlin, and G. BROGREN, Göteborg, for their interest in this work.

## Appendix

In estimating the energy dependency of nuclear reaction cross sections, the exact expression for the GAMOW factor has to be used. Because the involved calculations are somewhat tedious, two auxiliary graphs are given in Figs. 4 and 5. The GAMOW factors in frequent use, e. g. in calculating decay times of radioactive nuclei, correspond to the approximation $g'\, e^{-g'}$ with $(2/\pi)\ \xi = 1$.

[10] E. SCHOPPER, cited by J. BIERSACK and K. E. ZIMEN, Z. Naturforschg. **16 a**, 852 [1961].

[11] E. B. PAUL and R. L. CLARKE, Canad. J. Phys. **31**, 267 [1953].